

Short communication

# Effect of milling methods on performance of Ni–Y<sub>2</sub>O<sub>3</sub>-stabilized ZrO<sub>2</sub> anode for solid oxide fuel cell

Hyoup Je Cho, Gyeong Man Choi\*

Fuel Cell Research Center and Department of Materials Science and Engineering, Pohang University of Science and Technology, Pohang 790-784, Republic of Korea

Received 1 August 2007; received in revised form 17 August 2007; accepted 30 September 2007  
Available online 18 October 2007

## Abstract

A Ni–YSZ (Y<sub>2</sub>O<sub>3</sub>-stabilized ZrO<sub>2</sub>) composite is commonly used as a solid oxide fuel cell anode. The composite powders are usually synthesized by mixing NiO and YSZ powders. The particle size and distribution of the two phases generally determine the performance of the anode. Two different milling methods are used to prepare the composite anode powders, namely, high-energy milling and ball-milling that reduce the particle size. The particle size and the Ni distribution of the two composite powders are examined. The effects of milling on the performance are evaluated by using both an electrolyte-supported, symmetric Ni–YSZ/YSZ/Ni–YSZ cell and an anode-supported, asymmetric cell. The performance is examined at 800 °C by impedance analysis and current-voltage measurements.

Pellets made by using high-energy milled NiO–YSZ powders have much smaller particle sizes and a more uniform distribution of Ni particles than pellets made from ball-milled powder, and thus the polarization resistance of the electrode is also smaller. The maximum power density of the anode-supported cell prepared by using the high-energy milled powder is ~850 mW cm<sup>-2</sup> at 800 °C compared with ~500 mW cm<sup>-2</sup> for the cell with ball-milled powder. Thus, high-energy milling is found to be more effective in reducing particle size and obtaining a uniform distribution of Ni particles.

© 2007 Elsevier B.V. All rights reserved.

**Keywords:** Solid oxide fuel cell Ni–Y<sub>2</sub>O<sub>3</sub>-stabilized ZrO<sub>2</sub> anode; High-energy milling; Particle size; Nickel distribution; Power density

## 1. Introduction

Solid oxide fuel cells (SOFCs) are considered as promising energy conversion systems due to their high efficiency and environmentally friendly operation. A SOFC unit cell is basically composed of three components: electrolyte, cathode and anode. The most common material used for the SOFC anode is Ni–YSZ (Y<sub>2</sub>O<sub>3</sub>-stabilized ZrO<sub>2</sub>) cermet [1]. High electrical conductivity, good electrochemical activity, and proper microstructure are required to achieve better anode performance [2]. These conditions are mainly related to the particle size, the Ni content, and the distribution of the constituent phases. Increasing the Ni content enhances the electrical conductivity. On the other hand, a higher Ni content may decrease the performance of the anode due to Ni coarsening and mismatch of thermal expansion coef-

ficients (TECs). With optimization of Ni and YSZ distribution in the anode, the amount of reaction sites will increase and the agglomeration of Ni particles can be inhibited [3–4].

The optimum microstructure of a Ni–YSZ anode cannot be easily obtained since the microstructure is strongly dependent on the powder preparation technique and the fabrication process. Therefore, many attempts have been made to synthesize Ni–YSZ composite powders by chemical or mechanical methods. Chemical methods that produce powders in a liquid or gas phase often yield better performance than the conventional, mechanical mixing methods such as ball milling [5–7]. On the other hand, the chemical processes are often complex and thus expensive.

In view of the convenience and the ease of commercialization, a mechanical method is usually more attractive than a chemical counterpart. The high-energy milling (HEM) method, which mills and mixes powders with ceramic balls in high-speed rotation or agitation, can be a promising method for the synthesis of good anode powders. Although the method was originally developed to prepare nano-materials in metallurgy, various types of

\* Corresponding author. Tel.: +82 54 279 2146; fax: +82 54 279 2399.  
E-mail address: [gmchoi@postech.ac.kr](mailto:gmchoi@postech.ac.kr) (G.M. Choi).

nano-composites and nano-particles have been synthesized by using or modifying the method [8]. It was also applied to the fabrication of solid state anodes used in Li-ion batteries [9]. Ni–YSZ composite powders have also been synthesized with HEM methods [10–13]. Although both planetary milling and attrition milling were often considered as the HEM methods, the difference is often made by the way high energy is generated. In planetary milling, grinding bowls rotate around their own axes while also orbiting around a central axis [10,11]. As a result, forces are exerted on the grinding balls and material that are constantly changing direction and amount. By contrast, in attrition milling a central shaft with arms continually stirs a slurry of particles and spherical media, and provides a means to vary the grinding energy [12,13].

In this study, the effects of HEM on Ni–YSZ anode performance are investigated by comparing them with those of ball milling. The ball-milling (BM) method is another very popular method in particle-size reduction and mixing. The effects of the two powder preparation methods are examined and compared by making pellets composed of composite powders and testing their performance in an electrolyte-supported cell and an anode-supported cell.

## 2. Experimental procedure

NiO powders (99.97%, Kojundo Chemical, Japan) and YSZ powders (TZ-8YS, 99.9%, Tosoh, Japan) were used as the starting powders to synthesize NiO–YSZ composite powders. The starting powders were selected since they are easily available and have typical particle sizes. The mean diameters of the raw powders and the milled composite powders were measured with a laser particle size analyzer (CILAS 1064, France). The mean particle size ( $D_{\text{mean}}$ ) of NiO and YSZ powders was determined to be  $\sim 1.5$  and  $\sim 1.0$   $\mu\text{m}$ , respectively. The particle size may be different from the values reported by the manufacturer and thus reflects the agglomeration of powders.

The BM and HEM procedures were separately applied to the same starting mixture of NiO and YSZ powders for comparison. In the BM method, NiO and YSZ powders were mixed in ethanol and milled with zirconia balls (10 and 5 mm) at 160 rpm for 12 h. HEM (MiniCer, Netzsch, Germany; attrition-mill type in this study) was performed in the same media with zirconia balls (0.4 mm diameter) at a rotation speed of 2500 rpm for 2 h. Thus, a much shorter milling time was used for the HEM than for the BM. The ball-milled and high-energy milled powders were named, respectively, as NY-1 and NY-2.

For the examination of Ni and YSZ distribution, the composite powders were die-pressed and sintered at 1400 °C for 4 h to fabricate pellets. The Ni distribution in the composite pellets was examined by means of an electron probe micro analyzer (EPMA). In order to examine the anode performance, the composite powders were coated on both surfaces of a supporting YSZ pellet (500- $\mu\text{m}$  thick,  $\sim 20$  mm diameter) by screen printing. The screen printing slurry was made by mixing the powder with alpha-terpineol, ethyl cellulose and ethylene glycol. The cell was fired at 1200, 1300 and 1400 °C for 3 h to see the effects of firing temperature on the microstructure. The microstructure

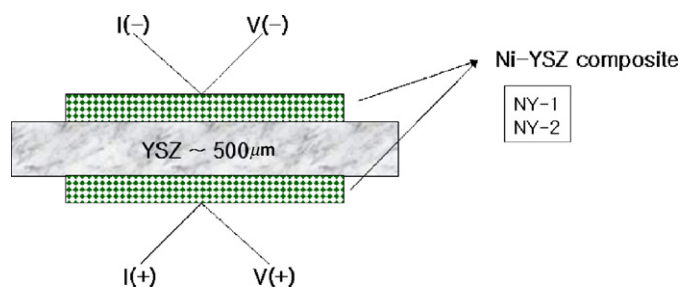


Fig. 1. Schematic view of electrolyte-supported, symmetric Ni–YSZ/YSZ/Ni–YSZ test cell.

of the anode was observed with a scanning electron microscope (SEM). A schematic of the configuration of the cell, and thus the anode characterization, is shown in Fig. 1. A semi four-probe method was used to eliminate the Pt lead-wire resistance. Pt paste (No.6082, Engelhard, USA) and Pt mesh (52 mesh, Alpha Aesar, USA) as a current-collector were attached to the sintered NiO–YSZ electrode. 97% $\text{H}_2$ –3% $\text{H}_2\text{O}$  gas was supplied as a reducing gas. The expected  $P_{\text{O}_2}$  was  $\sim 10^{-22}$  atm at 800 °C. Electrochemical testing of cell performance was carried out after 5 h reduction in the 97% $\text{H}_2$ –3% $\text{H}_2\text{O}$  gas atmosphere at 800 °C. An impedance analyzer (Solartron Instruments 1260, UK) was used to evaluate the electrode resistance and ohmic resistance. The impedance spectra were obtained under open-circuit conditions with an amplitude of 0.5 V in the frequency range 0.1 Hz–50 kHz.

Anode-supported cells were also fabricated using NY-1 or NY-2 anode powders. The supporting anode was uniaxially pressed to form a disc-shaped sample with a  $\sim 1$  mm thickness after sintering. Twenty and 15 wt.% of corn starch, respectively, were added as a pore former for the HEM and the BM anode substrates. The different amount of starch was used to obtain a similar sintering density. An anode functional layer of  $\sim 30$   $\mu\text{m}$  thickness was screen printed on a supporting anode of the same composition. No starch was added in the anode functional layer. An electrolyte layer of 10  $\mu\text{m}$  thickness (after sintering) was subsequently screen printed on the top of the anode functional layer. The cell was co-fired at 1300 °C for 3 h in air. The relative sintered density of both supported anodes was  $\sim 60\%$  after co-firing the cell in air. LSM ( $(\text{La}_{0.85}\text{Sr}_{0.15})_{0.98}\text{MnO}_3$ , NEXTECH, USA) powder was mixed with YSZ powder in a 6:4 weight ratio in ethanol and ball milled for 12 h with zirconia balls to prepare a LSM–YSZ composite cathode. The LSM–YSZ slurries were screen printed to produce a  $\sim 40$   $\mu\text{m}$ -thick cathode layer after sintering and additionally fired at 1100 °C for 3 h. The anode-supported cell was glass sealed to an alumina tube for the power test. The cells were characterized at 800 °C with 97% $\text{H}_2$ –3% $\text{H}_2\text{O}$  gas (100 cc  $\text{min}^{-1}$ ) as a fuel and air (open air) as an oxidant gas.

## 3. Results and discussion

The particle-size distributions of two composite powders after milling were measured and the results are given in Fig. 2. Both powders show reduced particle sizes compared with the starting powders ( $\sim 1.5$  and  $\sim 1.0$   $\mu\text{m}$  for NiO and YSZ,

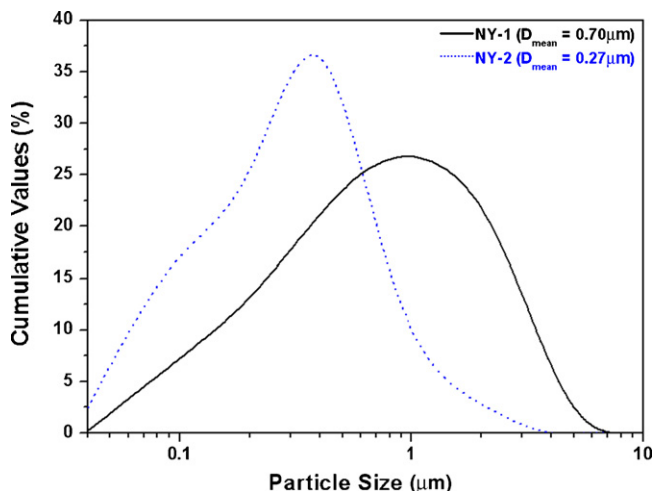


Fig. 2. Particle-size distribution of two composite powders determined by laser particle size analyzer. High-energy milled powder (NY-2) shows a smaller particle size and a narrower distribution.

respectively). The HEM powder (NY-2) has a much smaller mean particle size ( $\sim 0.27 \mu\text{m}$ ) than the BM powder (NY-1) ( $\sim 0.70 \mu\text{m}$ ) when the same starting powders are milled. The HEM powder also has a sharper distribution of particle size than the BM powder. Thus, the use of HEM powder is expected to improve the anode performance.

The distribution of Ni particles for two pellets made from the composite powders examined with EPMA is presented in Fig. 3. The bright area represents the Ni-rich area. The pellet made with the HEM powder has a smaller particle size and also a more uniform distribution of Ni particles compared with the pellet made with BM powder. This shows that the BM method has a limit on the reduction of particle size and the Ni dispersion. Thus BM may not be a suitable method to synthesize the anode composite. As a result, the use of HEM powder is expected to exhibit better cell performance in this experiment.

Impedance spectra of YSZ-supported cells with NY-1 and NY-2 anodes were measured at  $800^\circ\text{C}$  and the results are shown in Fig. 4. Each cell consists of two symmetric Ni–YSZ electrodes which are exposed to the same atmosphere ( $97\%\text{H}_2\text{-}3\%\text{H}_2\text{O}$  gas). The ohmic resistance of the two cells is similar. As

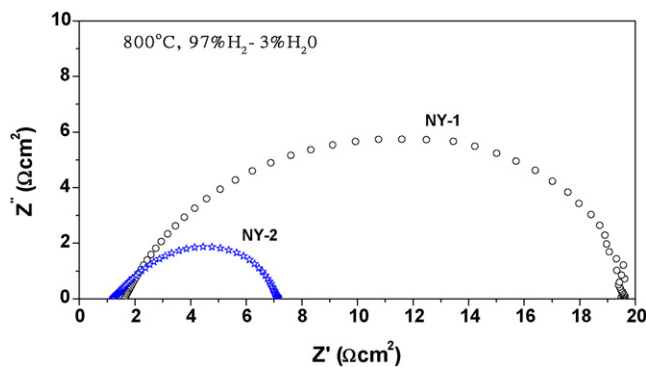


Fig. 4. Impedance spectra of YSZ cells with two symmetric composite electrodes measured at  $800^\circ\text{C}$  in  $97\%\text{H}_2\text{-}3\%\text{H}_2\text{O}$  gas atmosphere. Both electrodes are sintered at  $1400^\circ\text{C}$  for 3 h. The smaller polarization resistance of NY-2 electrode is attributed to smaller particle size and the uniform distribution of Ni.

expected, the electrode made from the HEM powder (NY-2) has a much lower polarization resistance ( $R_p \sim 6 \Omega \text{cm}^2$ ) than that made from BM powder (NY-1) ( $R_p \sim 18 \Omega \text{cm}^2$ ). Although both values are relatively large for the Ni–YSZ anode, this is due to the difference in the measurement conditions. In this study, the impedance analysis is carried out under a zero current condition and under no chemical or electrical potential gradient. Thus the current test conditions (one chamber) may be different from those of a real cell (two chambers) under a potential gradient. A much reduced  $R_p$  is expected in a real cell. Nevertheless, the trend in the  $R_p$  (Fig. 4.) should have a reasonably good correlation in the two conditions.

The sintering temperature is also an important factor affecting the particle size and the performance of the electrode. Thus it is necessary to compare the microstructure and the performance of electrodes sintered at different temperatures. Impedance spectra of YSZ cells with NY-1 (BM) and NY-2 (HEM) electrodes sintered at  $1200$ ,  $1300$  and  $1400^\circ\text{C}$ , measured at  $800^\circ\text{C}$  are shown in Fig. 5a and b, respectively. All impedance spectra shown in Fig. 5b are smaller than those in Fig. 5a. This indicates that the NY-2 (HEM) electrode has a smaller  $R_p$  than the NY-1 (BM) electrode at all temperatures. In addition, the electrode sintered at  $1300^\circ\text{C}$  has the lowest  $R_p$  for both NY-1 ( $\sim 8.5 \Omega \text{cm}^2$ ) and NY-2 ( $\sim 2 \Omega \text{cm}^2$ ) samples. The electrode fabricated with HEM

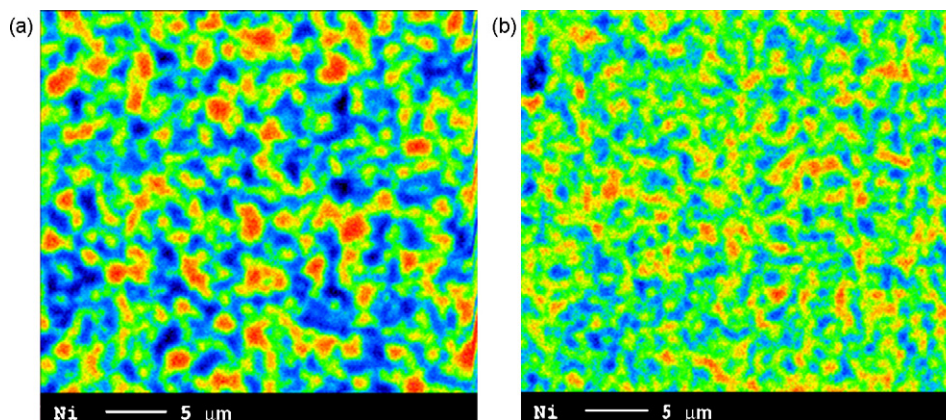


Fig. 3. Ni and YSZ particle distribution of pellets examined by EPMA mapping. Pellets made by using (a) NY-1 (ball-milling) and (b) NY-2 (high-energy milling) powders. Bright areas represent Ni-rich areas. NY-2 shows a more uniform distribution of Ni.

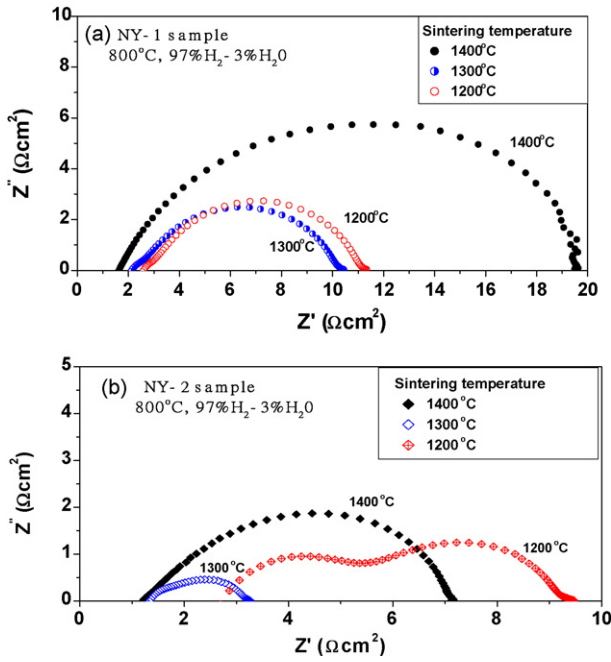


Fig. 5. Comparison of impedance spectra measured at 800 °C in 97% $H_2$ -3% $H_2O$  gas atmosphere of (a) NY-1 and (b) NY-2 electrodes sintered at 1200, 1300, and 1400 °C. Note scales in (a) and (b) are different.

powder (NY-2) and sintered at 1300 °C reports the smallest  $R_p$  ( $\sim 2 \Omega cm^2$ ). The firing or the sintering temperature of 1400 °C may be too high to maintain the fine particle size for both samples and may have resulted in the high  $R_p$  values ( $\sim 18$  and  $\sim 6 \Omega cm^2$  for NY-1 and NY-2, respectively). A temperature of 1200 °C may be too low to form good contacts between particles ( $R_p = \sim 9$  and  $\sim 7 \Omega cm^2$  for NY-1 and NY-2, respectively). The largest ohmic resistance values are found with 1200 °C sintered NY-1 and NY-2 samples. It is also noted that the impedance diagram for the NY-2 sample sintered at 1200 °C clearly displays

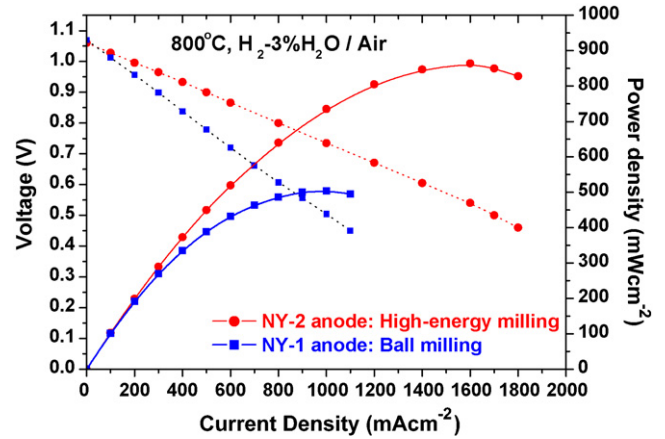


Fig. 7. Performance of anode-supported cell tested at 800 °C with 97% $H_2$ -3% $H_2O$  gas as a fuel gas and air as an oxidant gas. The higher maximum power density is shown for cell with high-energy milled, anode powder.

two arcs, and the 1300 °C data also give some indication of two arcs. This behaviour is not seen in the data for the NY-1 sample. Although the observation is not clearly understood, the shape of the impedance curve may be determined by the relative difficulties of charge transfer, gas phase diffusion, and/or gas adsorption reactions [2]. The modifications of particle size and distribution have clearly affected the relative contribution of the reactions.

In order to explain the impedance results, the microstructures of fired anodes are compared in Fig. 6. The particles sintered at 1400 °C are the largest and may possibly be too coarse for the good anode performance. The particles sintered at 1200 °C are the smallest and probably do not make good contact with each other. In order to understand fully this phenomenon, further studies on the effect of sintering temperature are necessary.

Since the anodic  $R_p$  values determined in a single atmosphere cannot be directly used under two atmosphere conditions and in order to test the effectiveness of milling methods on real

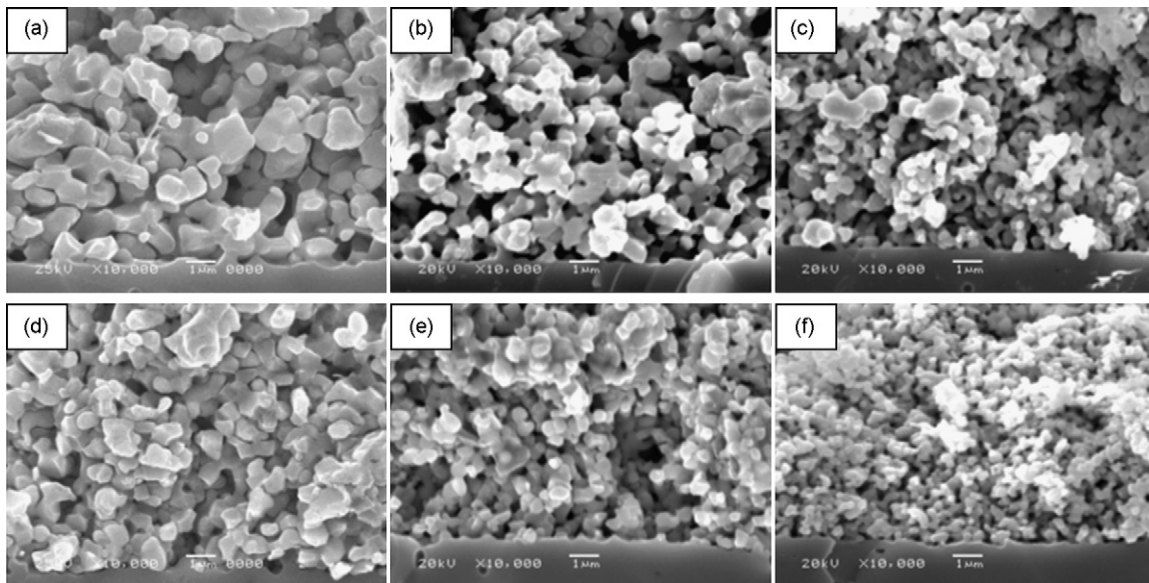


Fig. 6. Scanning electron micrographs of various electrodes: NY-1 samples sintered at (a) 1400, (b) 1300 and (c) 1200 °C, NY-2 samples sintered at (d) 1400, (e) 1300 and (f) 1200 °C. (Bar = 1  $\mu m$ ).

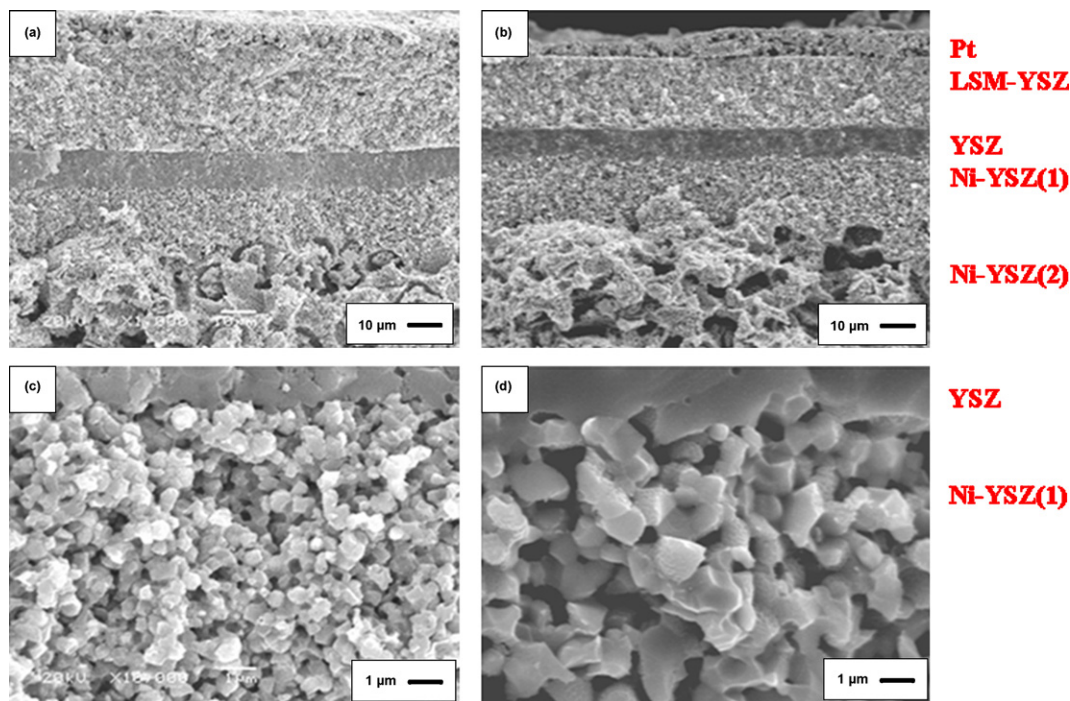


Fig. 8. Anode-supported cells fabricated by using either HEM or BM anode powders. Pt/LSM-YSZ/YSZ/Ni-YSZ(1)/Ni-YSZ(2) stacking structure is shown for two unit cells made by using (a) HEM and (b) BM anode powders. Anode functional layers (Ni-YSZ(1)) are shown for (c) HEM and (d) BM anodes. (Bar = 10  $\mu\text{m}$  for (a) and (b), bar = 1  $\mu\text{m}$  for (c) and (d)).

cells, anode-supported unit cells were fabricated using NY-1 or NY-2 anode powders. The performance of the two unit cells is given in Fig. 7. The anode-supported structure was co-sintered at 1300 °C. The temperature was selected since the lowest anodic  $R_p$  was observed, as shown in Fig. 5, with this sintering temperature. The maximum power density of the unit cell prepared with HEM powder is  $\sim 850 \text{ mW cm}^{-2}$  at 800 °C, compared with  $\sim 500 \text{ mW cm}^{-2}$  for that using BM powder. Since both the cathode and electrolyte are fabricated similarly for the two samples, the increased power density of the cell with the HEM powder is attributed to the particle size and the distribution of Ni and YSZ powders. Similar enhancement in cell performance due to the HEM method has been reported previously [13]. In order to determine the origin of the difference in performance, the microstructures of the cells were examined and compared, as shown in Fig. 8. The Pt/LSM-YSZ/YSZ/Ni-YSZ(1)/Ni-YSZ(2) stacking structure is clearly seen for two unit cells made by using HEM and BM anode powders (Fig. 8a and b). The Ni-YSZ(1) is an anode functional layer and the Ni-YSZ(2) is a supporting anode layer, respectively. From comparison of the microstructures of anode functional layers, it is concluded that the HEM anode (Fig. 8c) has a much smaller particle size ( $<1 \mu\text{m}$ ) than the BM anode ( $>1 \mu\text{m}$ ) (Fig. 8d). The difference in particle size is maintained even after sintering at 1300 °C.

This result implies that the HEM method is a simple, but effective, method to improve the anode and thus the cell performance through particle-size reduction and uniform particle distribution. A further enhancement of power density is expected through the optimization of the microstructures of the anode and the cathode.

#### 4. Conclusions

A high-energy milling (HEM) method produced a much smaller particle size and a better distribution of powder constituents than a ball-milling (BM) method, as revealed by the microstructures of composite pellets. The effects of milling methods are further examined by fabricating and testing a symmetric electrolyte-supported cell and an anode-supported cell.

An electrolyte-supported cell with symmetric Ni-YSZ composite electrodes made by using the HEM powder showed a much smaller polarization resistance compared with a cell using electrodes made from BM powder. The maximum power density of the anode-supported cell prepared with HEM powder is also higher. Thus, compared with the BM method, the HEM method is a more effective in reducing the particle size and obtaining a more uniform distribution of Ni particles. The electrode has to be sintered at a proper temperature (in this study, 1300 °C) to prevent coarsening of the particles during sintering and to enhance the electrical contacts between particles.

#### Acknowledgement

This research was supported by a grant (AC2-101) from Carbon Dioxide Reduction Sequestration Research Center, one of the 21st Century Frontier Program funded by the Ministry of Science and Technology of Korean government. High-Energy Milling was performed with the help of Prof. D.H. Yoon of Young Nam University, Korea.

**References**

- [1] N.Q. Minh, *J. Am. Ceram. Soc.* 76 (1993) 563–588.
- [2] N.Q. Minh, T. Takahashi, *Science and Technology of Ceramic Fuel Cell*, Elsevier, NY, 1995, pp. 147–161.
- [3] D.S. Lee, J.H. Lee, J. Kim, H.W. Lee, H.S. Song, *Solid State Ionics* 166 (2004) 13–17.
- [4] H. Itoh, T. Yamamoto, M. Mori, *J. Electrochem. Soc.* 144 (1997) 641–646.
- [5] T. Tukai, S. Ohara, M. Naito, K. Nogi, *Powder Technol.* 132 (2003) 52–56.
- [6] S.K. Pratihari, A.D. Sharma, H.S. Maiti, *Mater. Chem. Phys.* 96 (2006) 388–395.
- [7] S. Li, R. Guo, J. Li, Y. Chen, W. Liu, *Ceram. Int.* 29 (2003) 883–886.
- [8] P. Baláža, E. Godočiková, L. Kril'ová, P. Lobotka, E. Gock, *Mater. Sci. Eng. A* 386 (2004) 442–446.
- [9] B.-C. Kim, K. Takada, N. Ohta, *Solid State Ionics* 176 (2005) 2383–2387.
- [10] H.S. Hong, U.-S. Chae, S.-T. Choo, K.S. Lee, *J. Power Sources* 149 (2005) 84–89.
- [11] H.S. Hong, U.-S. Chae, S.-T. Choo, *J. Alloys Compd.*, in press.
- [12] T. Fukui, K. Murata, S. Ohara, H. Abe, M. Naito, K. Nogi, *J. Power Sources* 125 (2004) 17–21.
- [13] H. Abe, K. Murata, T. Fukui, W.-J. Moon, K. Kaneko, M. Naito, *Thin Solid Films* 496 (2006) 49–52.